Self-sustained biochemical oscillations and waves with a feedback determined only by boundary conditions

E. B. Postnikov,* A. Yu. Verisokin, and D. V. Verveyko
Department of Theoretical Physics, Kursk State University, Radishcheva Street 33, 305000 Kursk, Russia

A. I. Lavrova†
Institute of Physics, Humboldt-University at Berlin, Newtonstr. 15, 12489 Berlin, Germany

(Received 26 November 2009; revised manuscript received 5 March 2010; published 17 May 2010)

We discuss the biochemical three-dimensional reaction-diffusion model, which does not provide temporal self-sustained oscillations via reaction terms. However, the self-sustained oscillations and waves could be obtained using the proper boundary conditions for systems with a finite thickness. We have carried out in our numerical simulation the results quite corresponding to the experimental ones. We discuss the range of models for which our approach is applicable.

DOI: 10.1103/PhysRevE.81.052901 PACS number(s): 82.39.−k, 02.30.Mv

I. INTRODUCTION

The recent interest in the traveling waves in biochemical systems goes from the fact that they play an important role in biological information processing. It is known that their velocity, form, and direction of propagation depend on the extra-cellular and intracellular distributions of metabolites, enzymes activity, and other factors, which determine cellular processes.

The glycolysis is a relatively well-studied experimental example presenting such phenomena: spatiotemporal dynamics has been investigated in a mixture of cells as well as in a yeast extract. Self-sustained behavior of the waves is studied in the so-called open spatial reactor [1,2]. It contains one-side fed gel reactor (OSFR), which consists of the gel-fixed yeast extract, where the reaction takes place in contact with continuously stirred tank reactor (CSTR). The last one provides the continuous substrate influx of substrate and product outflow.

Usually, the mathematical models providing the traveling waves and other patterns do not take into account a reactor thickness. However, a more precise description of chemical reactors should consider a finite volume of their parts [3]. Moreover, it has been shown in [4] that the relaxation oscillations can emerge even in the case of nonoscillating itself chemical reactions due to volume perturbation or shape changes.

Additionally, the spatiotemporal patterns can be induced by an exchange of reagents sufficiently determined by the boundary between reactors. The well-known example of such a behavior is the generation of wave trains in the distributed FitzHugh-Nagumo system with inhomogeneous boundary conditions [5]. However, this example deals with the excitable reaction containing positive and negative feedback within the reaction terms.

At the same time, these terms can physically belong to the different parts of a reactor in the case of glycolytic experiment [1,2]. Thus, we need to study the situation which has not been considered before: the monotone nonexcitable nonoscillating reaction in a combination with the proper boundary conditions for reagents.

That allows us to obtain temporal oscillations as well as traveling waves. Finally, we compare our numerical results with experimental data and discuss the mechanisms of the wave propagation in the presented system.

II. RESULTS

A. Onset of oscillations

As a basis for our investigations we have modified two-variable Selkov system [6] extended with diffusion [7],

$$\partial_t x = D_1 \nabla^2 x + \nu - xy^2, \tag{1}$$

$$\partial_t y = D_2 \nabla^2 y - wy + xy^2. \tag{2}$$

Here, x is a concentration of the substrate adenosine triphosphate (ATP), which completely transforms into the product adenosine diphosphate (ADP) with a concentration denoted by y; ν and w are the parameters which determine the substrate influx and product outflow correspondingly [6]. Additionally the diffusion coefficients are supposed to be equal and normalized to unity. Although the Selkov model is quite simple, it has been shown recently [8,9] that it reproduces and explains some complex spatiotemporal patterns quite satisfactory.

However, Eqs. (1) and (2) used in the cited papers formally combine in the right-hand-side terms describing exchange processes simultaneously with the reaction terms, i.e., without taking into account a reactor thickness. Moreover, recently the simplified situation has been considered where the product flows out of the reaction but not out of the gel as is observed in experiment.

We consider the situation where the exchange of reagents with outer media takes place through the OSFR boundary only. This implies that the reaction terms in Eqs. (1) and (2) should be subdivided into two groups. The first one consists only of the terms corresponding to the irreversible chemical

*postnicov@gmail.com
†aurebours@googlemail.com

reaction in the gel bulk. It will be kept in PDE. The second group collects the terms describing substrate influx (ν) as well as product degradation and outflow (wy) through the plane $z=0$ in the normal direction. For the reason mentioned above, they will be associated with the boundary conditions on the penetrable part of OSFR. As have been mentioned above the excess substrate is completely consumed inside a bulk during percolation through the gel-fixed yeast extract via the glycolytic reaction. Thus, there is no outflow outside. Conversely, there exists an excess of the product, which needs to be taken off through the OSFR/CSTR boundary. Let us consider a uniform constant influx as a simple case. In this situation, the functions will depend only on a z coordinate. As a result, the desired system takes the form

$$\partial_t x = \partial_z^2 x - xy^2, \tag{3}$$

$$\partial_t y = \partial_z^2 y + xy^2, \tag{4}$$

with the boundary conditions

$$\partial_z x|_{z=0} = -\nu, \quad \partial_z y|_{z=0} = wy, \tag{5}$$

at the bottom of the reactor where the normal coincides with the negative direction of z axes, and impenetrable conditions elsewhere.

Now the Eqs. (3) and (4) have an extremely reduced form: they describe only a unidirectional reaction without feedback leading to a limit-cycle solution. For this reason similar equations considered in [10] were rejected there, although they adequately reproduce chemical reaction and spatial bistability.

Therefore, the desired oscillatory property can be induced only by interactions at the bottom boundary. To derive the corresponding onset condition, it is useful to introduce the full concentration $c=x+y$. It follows from the sum of Eqs. (3) and (4) that this function c admits the simple diffusion equation $\partial_t c=\Delta c$. Its flux through the bottom boundary is determined by the combination $\partial_z c=wy-\nu$ at $z=0$. Therefore, the steady state corresponding to $y(0)=\nu/w$ produces null flux through the boundaries and the steady-state uniform distribution of the full concentration of substrate and product $c=c_s$. At the same time, substituting $x=c-y$ into Eq. (4) we get the spatially nonuniform steady-state distribution $y_s(z)$ as a solution of the nonlinear eigenvalue problem

$$\partial_z^2 y + (c_s - y_s)y_s^2 = 0, \tag{6}$$

with the boundary conditions

$$\partial_z y_s|_{z=0} = \nu, \quad \partial_z y_s|_{z=L} = 0, \quad y_s|_{z=0} = \nu/w. \tag{7}$$

To find the bifurcation point for a loss of stability, one can consider the small parallel displacement $\xi(t)$ from the steady-state curve: $y(z,t)=y_s(z)+\xi(t)$. That gives the linear equation

$$d_t\xi = -(3y_s - 2c_s)y_s\xi.$$

Since $y_s(z)$ is a monotonic function growing from $z=0$ to $z=L$, the desired condition is $3y_s(L)=2c_s$. If $3y_s(z)>2c_s$ for all $z\in[0,L]$, any small displacement will exponentially decrease and it will exponentially increase otherwise. The irreversible reaction (3) and (4) limits this growth and turns it into concentration decay. Then the process repeats periodically. Figures 1 and 2 present the results of numerical simulations [11]. Figure 1 presents the temporal oscillations in the boundary points. The initial values $y(0)=1.5$, $c(0)=2.24$ are taken as corresponding to the uniform initial distribution along the whole layer thickness. In this figure we can see that the system starting from initial conditions reaches the limit cycle.

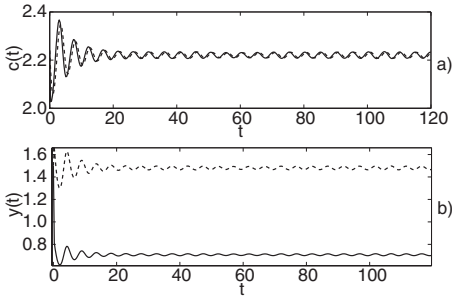

FIG. 1. The time dependences that correspond to the transient approaching stable limit cycles for (a) total concentration of reagents and (b) product taken in the points $z=0$ (solid line) and $z=L$ (dashed line). The parameters $L=1$, $w=2$, and $\nu=1.415$ are slightly smaller than the bifurcation values.

Figure 2 demonstrates the spatial envelopes of distributions for the reactants separately and their total concentration. One can see that the symmetry breaking of the total concentration distribution induces the oscillating process. The variation of the product concentration leads to the change of sign of boundary influx for the concentration $\partial_z c=wy-\nu$. This process realizes a negative feedback.

Thus, the presence of a finite reactor thickness can lead to new mechanisms for generation of self-sustained oscillations. This fact allows us to control their emergence more flexibly.

Figure 3 presents the analysis of the three parameters (ν,w,L) on the onset of oscillations determined by the eigenvalue problem (6) and (7). The oscillatory regime exists in some small range of parameters on the left of these curves, i.e., for smaller values of L and w consequently for a fixed ν. One can see that the growth of OSFR height induces the decrease in the influx value if the outflow rate is constant. Asymptotically ν scales as L^{-2} [dashed black line in the Fig.

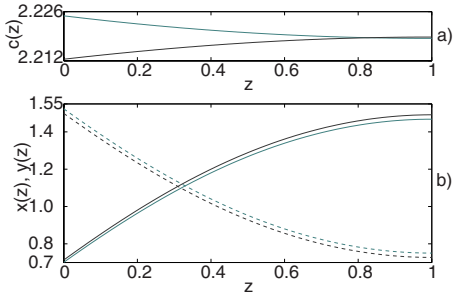

FIG. 2. (Color online) The maximal and minimal envelope distributions for (a) total concentration of reagents, and (b) product (solid lines) and substrate (dashed lines). The parameters are the same as in Fig. 1. The concentration oscillates between values corresponding to black and gray lines.

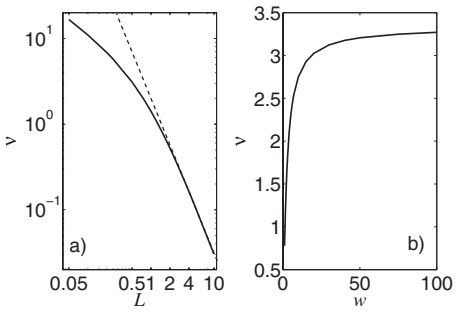

FIG. 3. Bifurcation curves: (a) the dependence of the influx value on the reactor height (the fixed value of outflow rate $w=2$); (b) the dependence of the influx value on the outflow rate (the fixed reactor height $L=1$).

2(a)]. This behavior is based on the fact that reagents redistribute over extremely large region and their distributions are sufficiently smoothed due to diffusive term in Eq. (6). Therefore, $y_s(0)=\nu/w$ is close to the value of $y_s(z)$ up to $y_s(L)=2c_s/3$ and Eq. (6) gives the asymptotic invariance $y_s \to L^{-2}y_s$, $z \to L^2 z$. On the other hand, the growth of outflow rate leads to saturation in the influx if the reactor height is fixed. Under this condition both boundary conditions are impenetrable [see Eq. (7) at $w \to \infty$] independently on ν.

B. Modeling of inward phase waves in three-dimensional glycolytic reactor

The presented results allow us to consider the problem of inward chemical wave emergence. It has been found in [1,2] that the two types of waves can propagate in this system. The waves propagating from the center of gel to the boundaries are called "outward waves." Otherwise, one can observe "inward waves." The last one is a nontrivial example which is studied now very actively [8,12]. Since there are two important experiments [2] revealing the origin of inward waves, we will focus on the inward waves modeling [13].

We assume that inward waves are induced by the inhomogeneous influx. In particular, we model this substrate inflow profile by an axially symmetric paraboloid, which has a minimum in the bottom center of OSFR: $\nu=\nu_0+4(\nu_1-\nu_0)r^2/d^2$, where ν_0 and ν_1 define the values of the influx in the center and at the borders, respectively.

We use the following parameters (see Table I). These parameters agreed with the bifurcation curve considered above. The renormalization $z/\sqrt{D} \to z$ leads to the renormalized value of thickness $L=2.9$. Therefore, the values of ν_0 and ν_1 located inside an oscillating domain (see Fig. 3).

TABLE I. The parameters which are used for the simulation.

Parameter	Value
Diameter of the disk	24
Thickness of the disk	1.3
Diffusion coefficient $D=D_1=D_2$	0.2
Influx parameter ν_0	0.359
Influx parameter ν_1	0.372
Outflow rate w	2
Gap width	1
Gap curvature radius	24

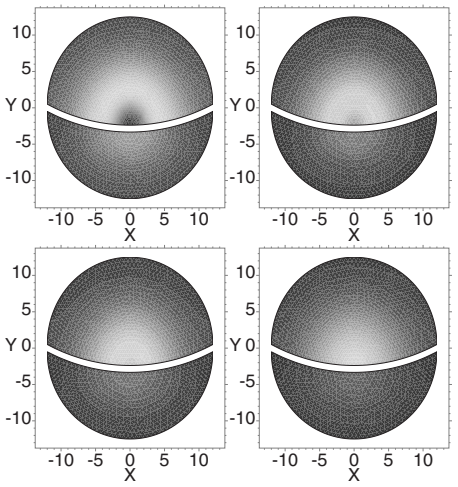

FIG. 4. The simulation of wave propagation in the reactor subdivided into two independent parts: the view from the top. Brighter regions correspond to the larger values of a product concentration as it presented in the experimental picture in Fig. 4.17 in [2].

The result is presented in the supplementary material [14]. Note that the simulation has been conducted within a whole disk. In order to present the details of wave propagation, one sector is cut out.

One can see that the process consists of three stages. During the first stage the substrate is diffusing from the bottom to top of OSFR, which results in a start of the reaction. It can be detected as a fast change in the product concentration expressed in the supplementary material [14] via pseudocolor scale. At the next stage one can observe the ring at the upper plane. It emerges due to increasing of the product outflux in the region of its high concentration [see Eq. (5)]. This ring moves to the disk center representing the inward wave. After a collapse of this wave the process repeats again.

In the further experiment the influence of an impenetrable barrier on the wave propagation has been studied [2]. It has been found that this barrier does not change the qualitative picture of ring-shaped waves starting from the border and approaching the center of disk (see Fig. 4.17 in [2] and the corresponding discussion there). This suggests that inwardly propagating waves are phase waves and propagate due to the phase-shifted oscillations.

To prove this conclusion within our PDE model, we have simulated the situation by the subdivision of the disk into two independent parts. The gap parameters presented in Table I are the same as in the experimental setup. Figure 4 shows the results of simulation taken at the same phases as in Fig. 4.17 in [2]. One can see that both parts of the reactor contain arcs (bright regions), which are the parts of the ring-shaped wave traveling to the reactor center. These arcs collapse simultaneously to the central point during the time. The final picture (Fig. 4, bottom left) presents the brightest spot in the center of whole reactor, in spite it consists of two parts. This is completely similar behavior to Fig. 4.17 in [2],

which the author of the cited work called "the waves, formed below the barrier, cross the barrier, and propagate to the upper part of the gel." The author considers this fact as an experimental proof for the assumption that inwardly propagating waves are phase waves and propagate due to the phase-shifted oscillations.

In our simulation, the inward waves are definitely phase waves formed by the inhomogeneous influx. Thus, this quite good correspondence between the experimental and model results confirms both the physical explanation of the phenomenon as well as an adequacy of the presented simple model.

III. DISCUSSION AND CONCLUSION

Thus, we have found that self-sustained oscillations can emerge in the systems, where only autocatalytic reaction exists. In our case, the required negative feedback can be replaced with the proper boundary condition. Namely, the third kind of boundary conditions provides a variable outflow of the product, which is conditioned by the concentration changes via reaction in a bulk. At the same time, the inhomogeneity of an influx allows us to obtain not only oscillations but traveling waves as well. It also determines their direction of propagation.

In general, it is important also for a study of spatiotemporal patterns in a large variety of chemical systems. Recently, Horváth *et al.* [15] considered the systematic way to design an experimental setup providing reaction-diffusion patterns. They argued that the procedure is based on reactions, which combine autocatalytic spatial bistability, spatiotemporal self-sustained oscillations, and asymmetry of reagents mobility. However, the system [15], as well as earlier [3,10], deals with the continuously stirred tank reactor in contact with the one-side fed gel reactor in the case of chemical reaction, which goes simultaneously in the both parts. For this reason one needs to have an independent reactive negative feedback to produce spatiotemporal oscillations.

At the same time, the glycolytic spatioextended experimental system can exhibit a large variety of spatiotemporal patterns [1,9], where different mechanisms can play a crucial role discussed in our work. Thus, the considered conditions provide enlarged possibilities for planning new experiments concerning the search of spatiotemporal patterns.

Finally, this approach can be applied to the description of processes in living systems, for example, cells. In this situation, biochemical traveling waves or stationary patterns inside the cytosole are excited by outer chemical stimuli acting on the membrane. There is an assumption that this fact plays an important role in cellular signal transduction and information processing [16].

[1] S. Bagyan, T. Mair, E. Dulos, J. Boissonade, P. De Kepper, and S. C. Müller, Biophys. Chem. **116**, 67 (2005).
[2] S. Vermeer, Ph.D. thesis, Magdeburg University, 2008; the full electronic text is freely available through Deutschen Nationalbibliothek, http://d-nb.info/995027714
[3] P. De Kepper, P. E. Dulos, J. Boissonade, A. De Wit Dewel, and P. P. Borckmans, J. Stat. Phys. **101**, 495 (2000).
[4] J. Boissonade, Phys. Rev. Lett. **90**, 188302 (2003).
[5] O. Nekhamkina and M. Sheintuch, Phys. Rev. E **73**, 066224 (2006).
[6] E. Sel'kov, Eur. J. Biochem. **4**, 79 (1968).
[7] J. Wolf and R. Heinrich, BioSystems **43**, 1 (1997).
[8] A. I. Lavrova, L. Schimansky-Geier, and E. B. Postnikov, Phys. Rev. E **79**, 057102 (2009).
[9] A. I. Lavrova, S. Bagyan, T. Mair, M. J. B. Hauser, and L. Schimansky-Geier, BioSystems **97**, 127 (2009).
[10] M. Fuentes, M. N. Kuperman, J. Boissonade, E. Dulos, F. Gauffre, and P. De Kepper, Phys. Rev. E **66**, 056205 (2002).
[11] MATLAB solvers bvp4c and pdepe are used for boundary value problem and one-dimensional simulation correspondingly. The first one generates mesh adaptively; 101-node uniform grid is applied for the second. The default relative (0.001) and absolute (10^{-6}) tolerance are used.
[12] X. Shao, Y. Wu, J. Zhang, H. Wang, and Q. Ouyang, Phys. Rev. Lett. **100**, 198304 (2008).
[13] FLEXPDE v. 5.0.22 applies Galerkin finite element methods, with quadratic tetrahedra. Implicit backward difference method with adaptive mesh and time step refinements is used. The default estimated relative spatial and temporal error is 0.002.
[14] See supplementary material at http://link.aps.org/supplemental/10.1103/PhysRevE.81.052901 for presenting results of 3D computer simulation of inward waves in OSFR.
[15] J. Horváth, I. Szalai, and P. De Kepper, Science **324**, 772 (2009).
[16] H. R. Petty, BioSystems **83**, 217 (2006).